JOURNAL OF APPLIED PHYSICS **107**, 093917 (2010)

Interlayer exchange coupling and current induced magnetization switching in magnetic tunnel junctions with MgO wedge barrier

Witold Skowroński,[1,a)] Tomasz Stobiecki,[1] Jerzy Wrona,[1] Karsten Rott,[2] Andy Thomas,[2] Günter Reiss,[2] and Sebastiaan van Dijken[3]
[1]*Department of Electronics, AGH University of Science and Technology, Al. Mickiewicza 30, 30-059 Kraków, Poland*
[2]*Thin Films and Physics of Nanostructures, Bielefeld University, 33615 Bielefeld, Germany*
[3]*Department of Applied Physics, Aalto University, P.O. Box 15100, FI-00076 Aalto, Finland*

(Received 27 January 2010; accepted 19 March 2010; published online 7 May 2010)

Current induced magnetization switching and interlayer exchange coupling (IEC) in sputtered CoFeB/MgO/CoFeB exchange-biased magnetic tunnel junctions with an extremely thin (0.96–0.62 nm) MgO wedge barrier is investigated. The IEC is found to be ferromagnetic for all samples and the associated energy increases exponentially down to a barrier thickness of 0.7 nm. Nanopillars with resistance area product ranging from 1.8 to 10 $\Omega\ \mu m^2$ and sizes of 0.13 μm^2 down to 0.03 μm^2 and tunneling magnetoresistance values of up to 170% were prepared. We found, that the critical current density increases with decreasing MgO barrier thickness. The experimental data and theoretical estimations show that the barrier thickness dependence of the spin transfer torque can largely be explained by a reduction in the tunnel current polarization at very small barrier thickness. © *2010 American Institute of Physics*. [doi:10.1063/1.3387992]

I. INTRODUCTION

High density and fast magnetic random access memory can be implemented using the spin transfer torque (STT) effect, i.e., free layer magnetization reversal induced by a high density spin-polarized current in a magnetic tunnel junction (MTJ). STT was introduced theoretically by Slonczewski[1] and Berger[2] and experimentally demonstrated in spin valve giant magnetoresistance (GMR)[3] and tunneling magnetoresistance (TMR) (Ref. 4) multilayer structures. Crucial issues of current induced magnetization switching (CIMS) in MTJs are a reduction in the critical current and resistance area (RA) product without a substantial decrease in TMR. For epitaxial MTJs, the dependence of the interlayer exchange coupling (IEC) (Refs. 5 and 6) and CIMS (Ref. 7) on MgO barrier thickness have recently been published. In this paper, we discuss the influence of MgO barrier thickness on the IEC energy and STT in textured magnetron sputtered MTJs with a very thin MgO wedge barrier.

II. EXPERIMENTAL

MTJs with a Ta(5)/CuN(50)/Ta(3)/CuN(50)/Ta(3)/PtMn(16)/$Co_{70}Fe_{30}$(2)/Ru(0.9)/$Co_{40}Fe_{40}B_{20}$(2.3)/wedge MgO(0.6–1)/$Co_{40}Fe_{40}B_{20}$(2.3)/Ta(10)/CuN(30)/Ru(7) (thickness in nm) structure were deposited in a Timaris PVD cluster tool system from Singulus Technologies. All metallic layers were deposited by dc magnetron sputtering, whereas the insulating MgO layer was grown by rf sputtering from a sintered MgO target. The MgO wedge was sputtered using linear dynamic deposition wedge technology. The base pressure before deposition was below 5×10^{-9} Torr. The Ar working pressure during MgO sputtering was 1 mTorr and the applied rf power density to the MgO target was fixed at 6.6 W/cm^2. This deposition condition resulted in (001) textured MgO layers (for details see Ref. 8). After deposition, the complete stack was annealed in a high-vacuum furnace for 2 h at 360 °C under an applied magnetic field of 10 kOe. The entire wafers were characterized electrically using a current in-plane tunneling (CIPT) method (Capres set-up)[9] and magnetically by magneto-optical Kerr effect (MOKE) magnetometry. On several test samples, the MgO barrier thickness was calibrated using x-ray reflectivity. Afterwards, the samples were cut into smaller pieces for patterning of MTJ nanopillars with different insulating barrier thickness. Using e-beam lithography, ion beam milling, and lift-off, the junctions were patterned into elliptical shapes with the long diameter parallel to the easy magnetization axis. The sizes of the MTJs were 160×250, 280×430, and 280×620 nm^2 (in this paper we discuss size 160×250 only). Magnetotransport measurement were carried out using constant voltage method. In order to measure CIMS curves a sequences of voltage pulses with different amplitude were applied. The pulse length varied from 1 ms up to 500 ms. In this paper, positive voltage indicates electron transport from the pinned bottom layer to the free top layer.

III. RESULTS AND DISCUSSION

A. TMR and RA product

Figure 1(a) depicts the TMR and RA product as a function of MgO thickness, measured using the CIPT method on unpatterned multilayer stack. For thick MgO barriers down to 0.75 nm, the change in the TMR value is relatively small (from 170% to 150%), indicating good barrier quality and an absence of pinholes. The RA product increases exponentially with MgO thickness. When the RA product is reduced to 1.5 $\Omega\ \mu m^2$ (which corresponds to an MgO thickness of about 0.7 nm) the TMR starts to drop. This can be explained

[a)]Electronic mail: skowron@layer.uci.agh.edu.pl.

 © 2010 American Institute of Physics

Downloaded 12 May 2010 to 130.233.204.212. Redistribution subject to AIP license or copyright; see http://jap.aip.org/jap/copyright.jsp

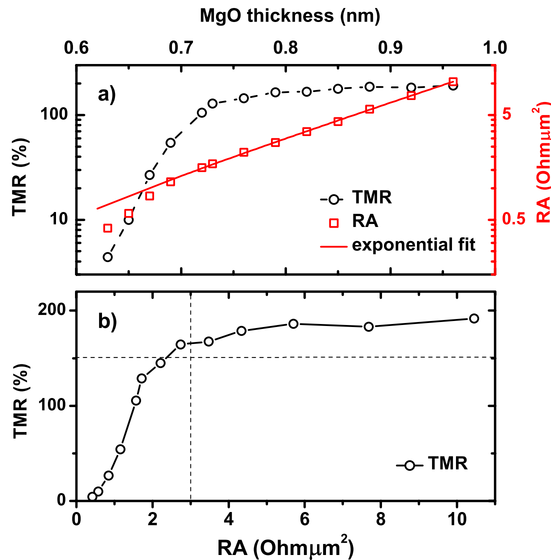

FIG. 1. (Color online) (a)TMR and RA product as a function of MgO barrier thickness measured on unpatterned multilayer stacks using CIPT. The RA product is measured with P aligned magnetic moments. (b) shows TMR ratio as a function of the RA product. The TMR exceeds 150% for MTJs with RA product greater then 3 Ω μm^2.

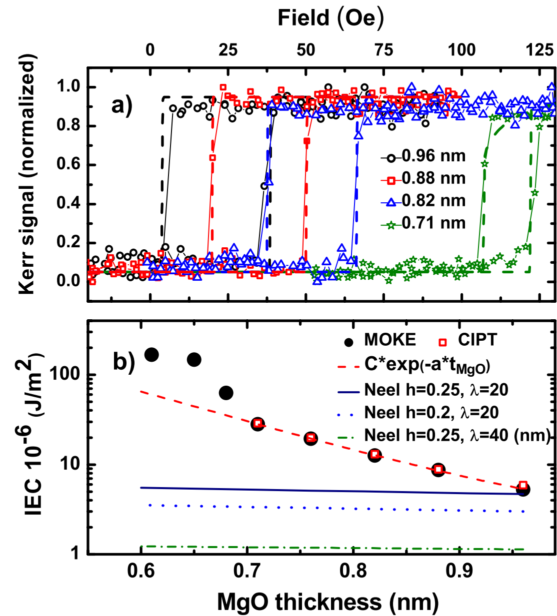

FIG. 2. (Color online) (a) Minor MOKE loops of the multilayer stacks with 0.96, 0.88, 0.81 and 0.71 nm MgO barriers and its theoretical fit and (b) IEC energy between the CoFeB-free and CoFeB reference layer as a function of MgO barrier thickness. The data can be fitted using an exponential function down to 0.7 nm. The estimated Néel coupling energy for different roughness parameters are smaller and less dependent on the barrier thickness than the experimental data.

by barrier imperfections which are also reflected by a change in the slope of the RA product versus MgO thickness curve. Additionally we plot TMR ratio as a function of RA product—Fig. 1(b).

B. IEC

Magnetic hysteresis loops of unpatterend multilayer stacks in high (major loop) and low (minor loop) field were measured using MOKE. Representative results of minor loops for selected MgO barrier thicknesses (0.96, 0.88, 0.82, and 0.71 nm) are presented in Fig. 2(a). Using the CIPT technique, similar results for magnetization reversal in the free layer were obtained. Both measurement techniques clearly show that minor loops are shifted toward positive field values, which indicates ferromagnetic coupling between the free and reference layer of the multilayer stack. Using the Stoner–Wohlfart surface energy model for exchange-biased spin-valves,[10] the coupling energy between the free and reference layer was calculated. The macrospin simulation results are shown in Fig. 2. Down to 0.7 nm MgO barrier thickness, the data can be fitted by an exponential function $J_{IEC} \propto \exp(-t_{MgO})$. For thinner barriers, however, additional effects due to e.g., pinholes become significant and the dependence of the coupling on MgO barrier thickness is no longer described by an exponential. As expected, the exchange coupling energies of other interfaces was found to be independent of barrier thickness. From major magnetic hysteresis loops, the following values were determined: exchange bias energy (PtMn/CoFe) $J_{EB}=0.19$ mJ/m^2 and synthetic antiferromagnet (SAF) coupling energy (CoFe/Ru/CoFeB) $J_{SAF}=-0.22$ mJ/m^2. These values are much larger than the coupling between the free layer and the reference layer and therefore ensure good pining of the bottom CoFeB electrode. Our result on the barrier thickness dependence of IEC contrasts the experiments by Faure-Vincent *et al.*[5] and Katayama *et al.*[6] on epitaxial Fe(001)/wedge MgO(001)/Fe(001) structures, as we do not observe the reported ferro-to antiferromagnetic exchange coupling transition with decreasing MgO barrier thickness. This discrepancy can be partially explained by the existence of dipolar ferromagnetic coupling known after Néel as the "orange-peel" coupling[11] in sputtered MTJ stacks, due to interface roughness, which might be smaller in epitaxially grown MTJs. Our results, however, cannot be explained by the existence of orange-peel coupling alone. We estimated the influence of the interface roughness using the model in Ref. 12. The roughness amplitude of the bottom CoFeB electrode after annealing was measured with AFM and do not exceed 0.25 nm. The roughness wavelength in the whole stack originates mainly from the buffer, in our case thick and smooth CuN/Ta.[13] We assume, that both amplitude and wavelength of the roughness do not depend on the MgO barrier thickness. Varying the roughness amplitude and wavelength of the CoFeB electrode in the range of $h=0.15-0.25$ nm and $\lambda=20-50$ nm, respectively,[8] and assuming the saturation magnetization $M_S=0.8$ MA/m, the maximum value of the Néel coupling energy is 5 μJ/m^2, which corresponds to the shift in the magnetic loop of 25 Oe. This value is much smaller than the loop shift in our measurements and therefore the majority of the shift is attributed to a direct ferromagnetic IEC across the MgO barrier.

Based on *ab initio* calculations of an ideal single crystal Fe(001)/MgO (001)/Fe(001) system, with a similar MgO barrier thickness range, Zhuravlev *et al.*[14] obtained the ferromagnetic IEC, exponentially decaying with MgO barrier thickness. However, the amplitude of the exchange coupling energy is of two orders of magnitude higher than in our experimental data. They showed that for junctions containing

Downloaded 12 May 2010 to 130.233.204.212. Redistribution subject to AIP license or copyright; see http://jap.aip.org/jap/copyright.jsp

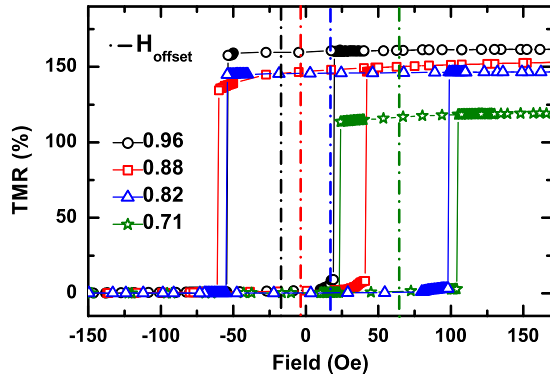

FIG. 3. (Color online) TMR minor loops of the MTJ nanopillars with different MgO thicknesses measured at 10 mV bias voltage. With decreasing barrier thickness the TMR ratio drops and the offset field increases due to IEC.

variable concentration of the oxygen vacancies or localized defect states, it is possible to reduce, or even change the sign of the exchange coupling energy.

In our experiment, during an annealing process the B atoms from CoFeB electrode can diffuse into the MgO barrier[15] (which is not the case in pure Fe electrodes used in experiment in Refs. 5 and 6), which can result in other exchange mechanisms. We believe that our results of ferromagnetic IEC in polycrystalline textured junctions FeCoB (001)/MgO (001)/FeCoB(001) can be understood on the basis of the band calculations of a non ideal single crystal junction.

C. CIMS

Representative TMR loops of the MTJ nanopillars with different MgO barrier thicknesses are shown in Fig. 3. The shift in the loop decreased in comparison to the unpatterned MTJ stack. The offset field in nanopillars is a result of the competition between ferromagnetic IEC and magnetostatic coupling at the edges of the magnetic layers.[16]

All MTJs exhibit clear CIMS. Figure 4 presents the voltage pulse duration (t_p) dependence of the critical current density (J_c) for junctions with a 0.96 nm thick MgO tunnel barrier, together with a typical example of resistance versus voltage loops measured in an external magnetic field that compensated the total interlayer coupling. According to the theoretical model of Refs. 17 and 18 based on Slonczewski's theory,[19] J_c can be expressed as

$$J_c = J_{c0}\left[1 - \left(\frac{2k_BT}{H_CM_SV}\right)\ln\left(\frac{t_p}{t_0}\right)\right], \tag{1}$$

where, J_{c0} is the intrinsic switching current density, H_C the coercive field, M_S the saturation magnetization, V the volume of the free layer, T is temperature and t_0 is the inverse of the attempt frequency, which was set to 1 ns. The experimental value of J_{c0} can be obtained by extrapolation of the switching current densities to $\ln(t_P/t_0)=0$. In our experiment, the results are: $J_{c0}^{+}=6.4\pm0.5\times10^6$ A/cm^2 for switching from the antiparallel (AP) to the parallel (P) state and $J_{c0}^{-}=-1.5\pm0.2\times10^7$ A/cm^2 for switching from P to AP. Theoretical, the value of the J_{c0} can be estimated using a phenomenological model[20]

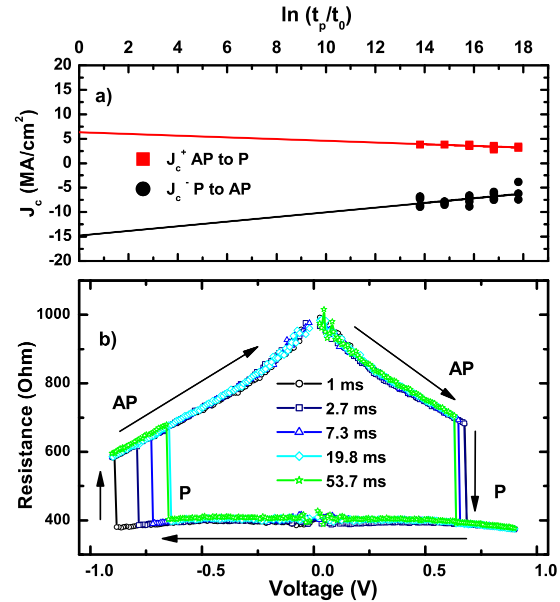

FIG. 4. (Color online) (a)Switching current density dependence on the pulse duration for a MTJ with 0.96 nm thick MgO barrier and (b) representative resistance vs voltage curves for different voltage pulse duration times.

$$J_{c0} = \frac{2e\alpha\mu_0M_St_F(H \pm H_K \pm H_D)}{\hbar\eta}, \tag{2}$$

where e is the electron charge, α is a damping constant, t_F is the thickness of the free magnetic layer, H, H_K, and H_D are external magnetic field, anisotropy field, and demagnetizing field, respectively, $\hbar$ is the reduced Planck's constant and η is the spin transfer efficiency. Assuming $\alpha=0.017$ [measured on the same samples using pulse inductive microwave magnetometry (PIMM) (Ref. 21)], $H_K \ll \mu_0M_S=2H_D=1$ T, $t_F=2.3$ nm, and $\eta=(p/2)/(1+p^2\cos\theta)$, where p is the spin polarization of the tunnel current derived from Julliere's formula[22] and $\theta=0°$ and 180° for switching from the P and AP state, respectively, the calculated values are $J_{c0}^{+}=7.7\times10^6$ A/cm^2 and $J_{c0}^{-}=-2.1\times10^7$ A/cm^2.

A similar experiment was performed on MTJs with thinner MgO barriers. The results are gathered in Fig. 5. The observed increase in the switching current density with decreasing tunnel barrier thickness is mainly explained by a reduction in the spin polarization p (Ref. 23) as illustrated by

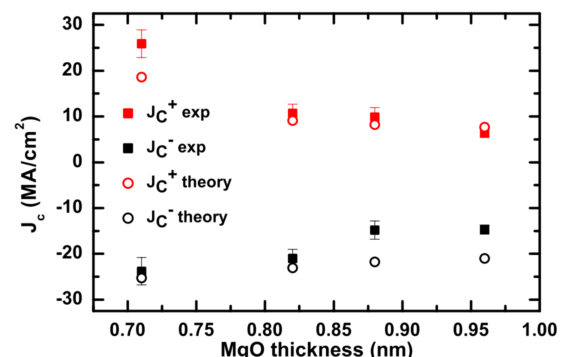

FIG. 5. (Color online) The switching current density for MTJs with different MgO barrier thickness. Theoretical values were calculated using Eq. (2) and TMR and PIMM results.

Downloaded 12 May 2010 to 130.233.204.212. Redistribution subject to AIP license or copyright; see http://jap.aip.org/jap/copyright.jsp

the decrease in TMR in Fig. 1. Figure 5 also shows theoretical values for J_{c0} that were calculated using Eq. (2). The spin polarization was estimated from the TMR ratio at low bias voltage using Julliere's formula, whereas the damping was determined from the PIMM. The difference in the asymmetry of the switching current densities between the junctions with a 0.71 nm (small asymmetry) and thicker (large asymmetry) MgO tunnel barrier is explained by a change in the damping constant, which also influences the switching current process. In our experiments, the junctions with a 0.71 nm MgO tunnel barrier exhibited α=0.03 and α=0.017 for the AP and P magnetization state, respectively, whereas junctions with a thicker barrier showed equal damping factors for both states.[21] The more detailed studies on damping mechanism in MgO wedge MTJs will be published elsewhere.

IV. SUMMARY

We have investigated IEC and CIMS in CoFeB/wedge MgO (0.96–0.62 nm)/CoFeB exchange-biased MTJs. In the unpatterned multilayer stacks the IEC was found to be ferromagnetic for all MgO thicknesses. Measurements on nanopillar junctions with an RA product ranging from 1.8 to 10 $\Omega\ \mu m^2$, sizes of 0.03 μm^2, and TMR values of up to 170%, indicated an increase in the switching current density with decreasing tunnel barrier thickness. This effect and the related reduction in switching asymmetry are mainly attributed to a decrease in the tunnel current polarization and a stronger damping in MTJs with very thin MgO barriers.

ACKNOWLEDGMENTS

We would like to thank Berthold Ocker and Juergen Langer of Singulus Technologies AG for their consulting and technical help with MgO wedge MTJs preparation. W.S. would like to thank the Foundation for Polish Science MPD Programme co-financed by the EU European Regional Development Fund. T.S. would like to express gratefulness for financial support to SPINSWITCH Project under Contract No. MRTN-CT-2006-035327. S.v.D. acknowledges financial support from the Academy of Finland for the ACTIVE-BAR Project.

[1] J. Slonczewski, J. Magn. Magn. Mater. **159**, L1 (1996).
[2] L. Berger, Phys. Rev. B **54**, 9353 (1996).
[3] E. B. Myers, D. C. Ralph, J. A. Katine, R. N. Louie, and R. A. Buhrman, Science **285**, 867 (1999).
[4] Y. Huai, F. Albert, P. Nguyen, M. Pakala, and T. Valet, Appl. Phys. Lett. **84**, 3118 (2004).
[5] J. Faure-Vincent, C. Tiusan, C. Bellouard, E. Popova, M. Hehn, F. Montaigne, and A. Schuhl, Phys. Rev. Lett. **89**, 107206 (2002).
[6] T. Katayama, S. Yuasa, J. Velev, M. Y. Zhuravlev, S. S. Jaswal, and E. Y. Tsymbal, Appl. Phys. Lett. **89**, 112503 (2006).
[7] R. Matsumoto, A. Fukushima, K. Yakushiji, S. Yakata, T. Nagahama, H. Kubota, T. Katayama, Y. Suzuki, K. Ando, S. Yuasa, B. Georges, V. Cros, J. Grollier, and A. Fert, Phys. Rev. B **80**, 174405 (2009).
[8] J. Wrona, J. Langer, B. Ocker, W. Maass, J. Kanak, T. Stobiecki, and W. Powroźnik, J. Phys.: Conf. Ser. **200**, 052032 (2010).
[9] D. C. Worledge and P. L. Trouilloud, Appl. Phys. Lett. **83**, 84 (2003).
[10] M. Czapkiewicz, M. Zoladz, J. Wrona, P. Wisniowski, R. Rak, T. Stobiecki, C. G. Kim, C. O. Kim, M. Takahashi, and M. Tsunoda, Phys. Status Solidi **241**, 1477 (2004) (b).
[11] L. Néel, Compt. Rend. **255**, 1676 (1962).
[12] J. C. S. Kools, W. Kula, D. Mauri, and T. Lin, J. Appl. Phys. **85**, 4466 (1999).
[13] W. Maass and Y. Huai, Semiconductor International **1**, 57 (2005).
[14] M. Y. Zhuravlev, E. Y. Tsymbal, and A. V. Vedyayev, Phys. Rev. Lett. **94**, 026806 (2005); M. Y. Zhuravlev, J. Velev, A. V. Vedyayev, and E. Y. Tsymbal, J. Magn. Magn. Mater. **300**, e277 (2006).
[15] J. C. Read, P. G. Mather, and R. A. Buhrman, Appl. Phys. Lett. **90**, 132503 (2007).
[16] H. Kubota, Y. Ando, T. Miyazaki, G. Reiss, H. Brueckl, W. Schepper, J. Wecker, and G. Gieres, J. Appl. Phys. **94**, 2028 (2003).
[17] H. Kubota, A. Fukushima, Y. Ootani, S. Yuasa, K. Ando, H. Maehara, K. Tsunekawa, D. D. Djayaprawira, N. Watanabe, and Y. Suzuki, Appl. Phys. Lett. **89**, 032505 (2006).
[18] J. Hayakawa, S. Ikeda, Y. M. Lee, R. Sasaki, T. Meguro, F. Matsukura, H. Takahashi, and H. Ohno, Jpn. J. Appl. Phys., Part 2 **45**, L1057 (2006).
[19] J. Slonczewski, Phys. Rev. B **71**, 024411 (2005).
[20] Y. Huai, M. Pakala, Z. Diao, D. Apalkov, Y. Ding, and A. Panchula, J. Magn. Magn. Mater. **304**, 88 (2006).
[21] S. Serrano-Guisan, W. Skowroński, J. Wrona, M. Czapkiewicz, T. Stobiecki, J. Langer, B. Ocker, G. Reiss, and H. W. Schumacher, Proceedings of the 11th MMM/Intermag Conference, Washington, USA, 18–22 January 2010.
[22] M. Julliere, Phys. Lett. A **54**, 225 (1975).
[23] H. Itoh, J. Phys. D **40**, 1228 (2007).

Downloaded 12 May 2010 to 130.233.204.212. Redistribution subject to AIP license or copyright; see http://jap.aip.org/jap/copyright.jsp